

SUPPORTING INFORMATION

Broadband Plasmonic Microlenses based on  
Patches of Nanoholes

*Hanwei Gao,<sup>‡</sup> Jerome K. Hyun,<sup>§</sup> Min Hyung Lee,<sup>‡</sup> Jiun-Chan Yang,<sup>‡</sup>*

*Lincoln J. Lauhon,<sup>§</sup> Teri W. Odom<sup>‡,§\*</sup>*

<sup>‡</sup> Department of Chemistry, <sup>§</sup> Department of Materials Science and Engineering

Northwestern University, Evanston, Illinois 60208, USA

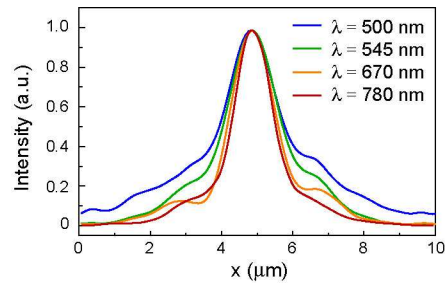


**Figure S1. Linescans at the focal planes of the confocal scanning optical images of 5- $\mu\text{m}$  patches in Fig. 1.** Reduced lateral dimensions of the focal spots were observed as the operating wavelength increased.

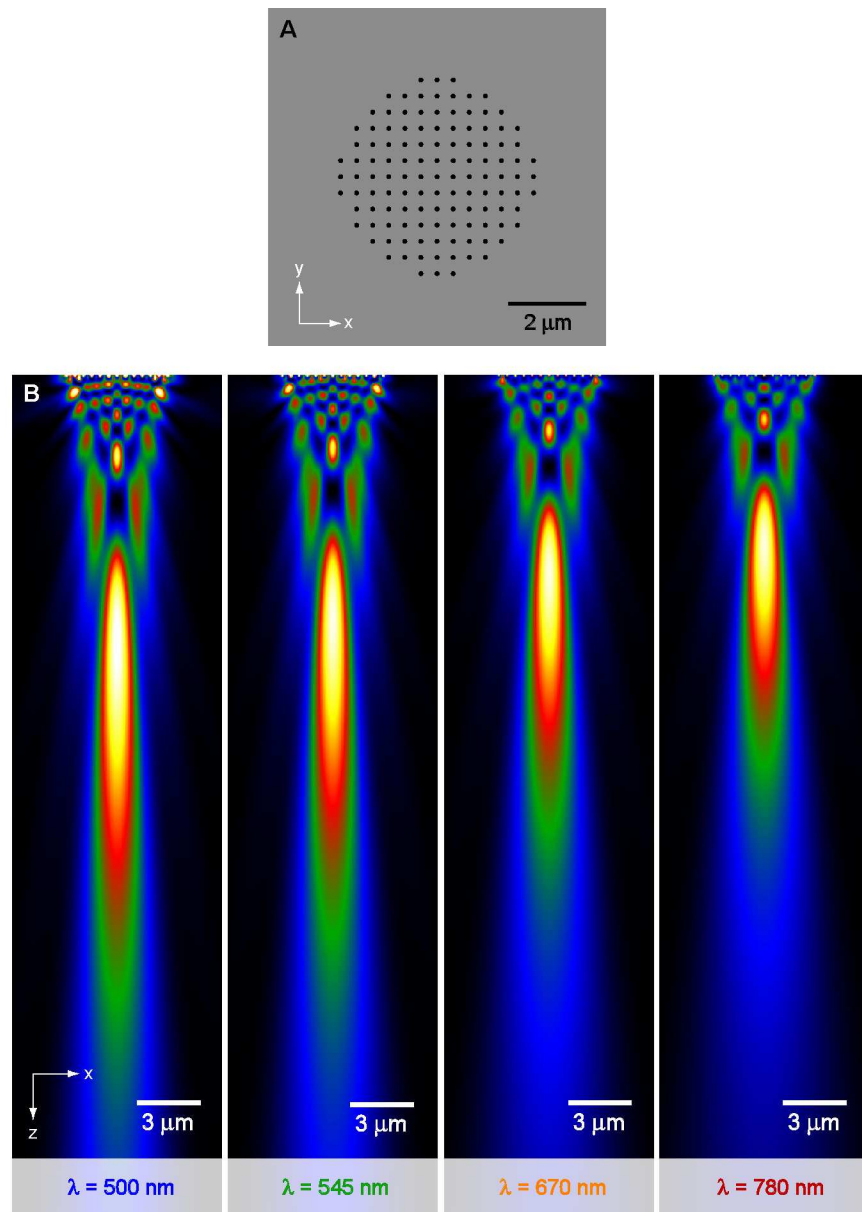


**Figure S2. Calculated optical field maps of light transmitted through 5- $\mu\text{m}$  patches.** (A) Nanoholes in patches were considered as electric-dipole point sources with  $a_0 = 400$  nm. The model does not take into account the size of the nanoholes, the thickness of the metal film, or the material properties  $\epsilon(\omega)$ . (B)  $x$ - $z$  cross-sections of calculated 3D electric field intensities at different wavelengths.

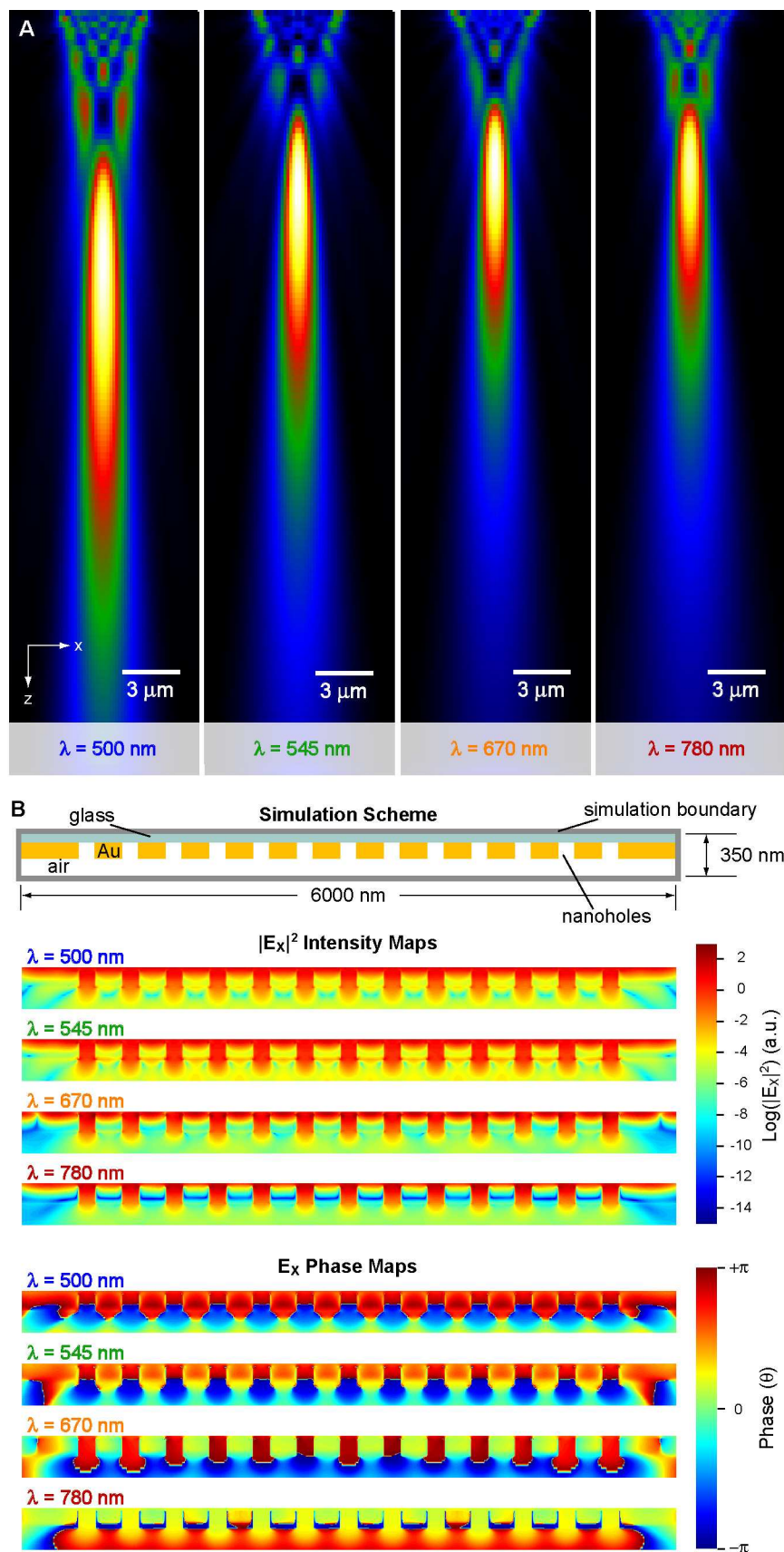


**Figure S3. FDTD calculations of optical transmission through 5- $\mu\text{m}$  patches.** Full-vector electromagnetic fields were simulated on 5- $\mu\text{m}$  patches using the FDTD method (Lumerical® software package). 150-nm diameter nanoholes were arranged on a 400-nm square lattice on a glass substrate.

The plane wave was incident from the glass side. The simulation volume was  $6\ \mu\text{m} \times 6\ \mu\text{m} \times 350\ \text{nm}$  with the patch surrounded by all absorbing boundary conditions. **(A)** Far-field electric field intensity maps. **(B)** Near-field electric field intensity and phase maps. Excellent agreement was achieved among the FDTD simulations, point-source calculation (**Fig. S2B**), and experiments (**Fig. 1**). In addition, the near-field distribution indicated that each nanohole transmitted electromagnetic fields with approximately equal amplitude and phase. The FDTD simulations validated the results of the point-source model and verified that no phase modulation was necessary to achieve focusing from the patches.

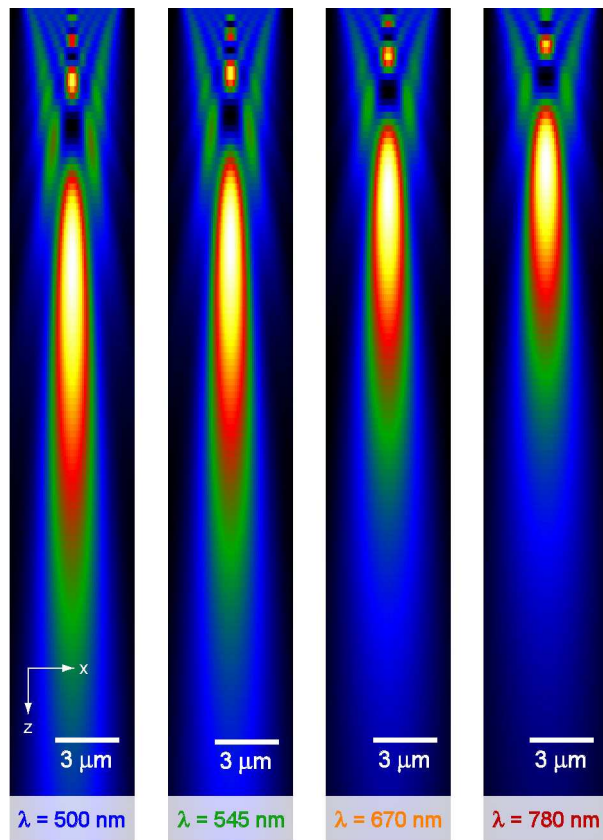


**Figure S4. FDTD simulated far-field transmission patterns through 5- $\mu\text{m}$  clear apertures in Au thin film.** The geometry of the main focal spot is similar to that from the 5- $\mu\text{m}$  patch of nanoholes.

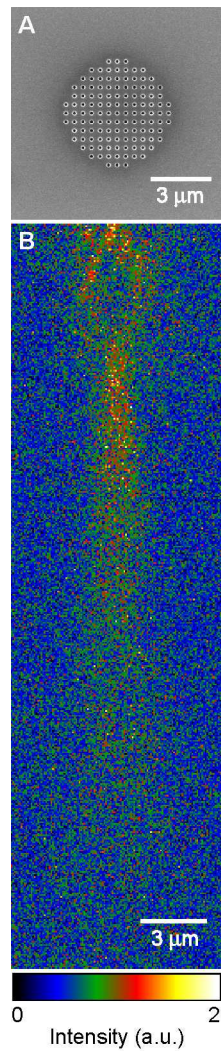


**Figure S5. Control experiment on a Ti patch.** (A) SEM of a Ti patch with identical geometric structure as the 5- $\mu\text{m}$  Au patch in Fig. 1. (B) The focusing effect was significantly obscured in this non-plasmonic material. Operating  $\lambda = 780$  nm.

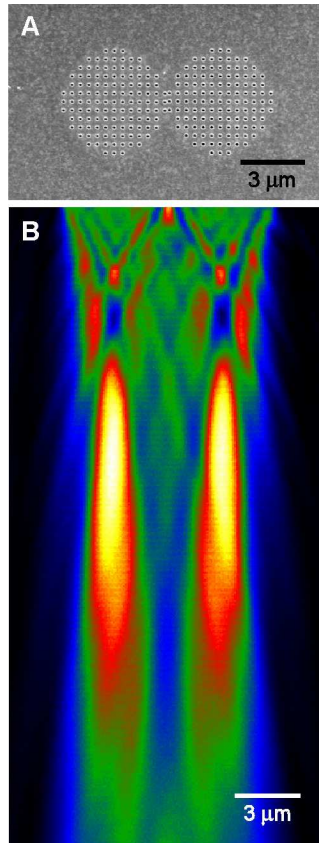


**Figure S6. Patches patterned edge-to-edge exhibit minimal cross-talk in the 3D optical pattern. (A)** SEM image of two 5-μm patches with no spacing in between patches. **(B)** Transmitted light through (A) showed minimal cross-talk between the beams. Operating  $\lambda = 545$  nm.



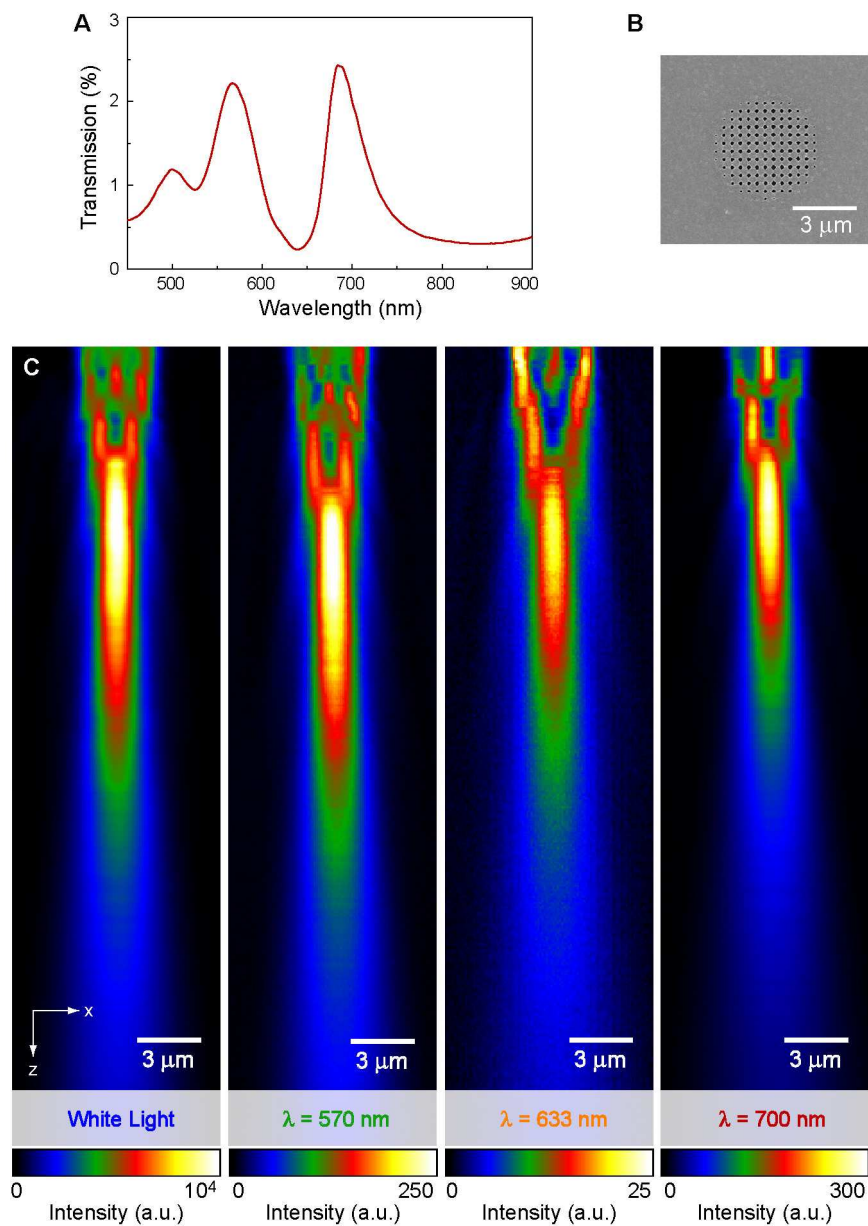


**Figure S7. Wafer-scale array of 5- $\mu\text{m}$  patches in Figure 4 can focus broadband visible light.** (A) Transmission spectra showed distinct plasmon resonances around 570 nm and 700 nm. The Au film was about 150 nm thick. The diameter of the nanoholes was 130 nm in the center of the patches and smaller on the perimeter. (B) SEM image of the patch. (C) Far-field optical intensity maps were measured using a conventional optical microscope under collimated ( $< 4^\circ$  divergence) wide-field illumination. Well-defined focal spots were observed at different wavelengths. The contrast and intensity is much higher at plasmon resonances (570 nm and 700 nm). The patches can also focus broadband illumination from a halogen lamp.

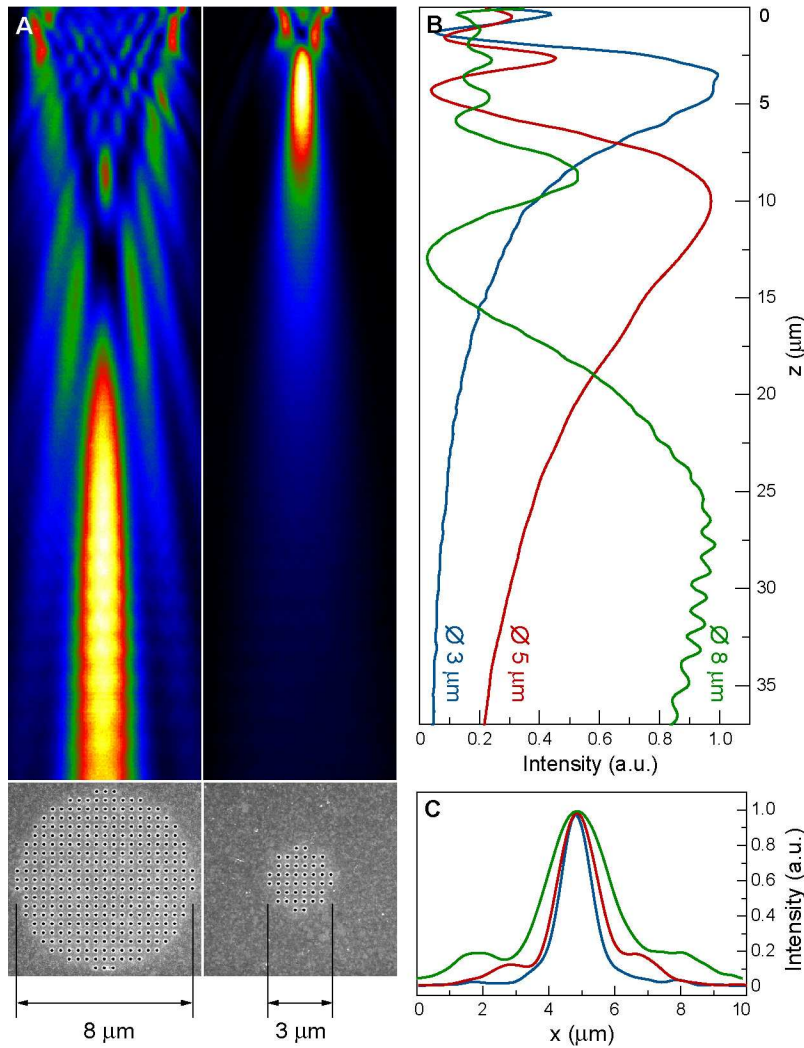


**Figure S8. The microlens focal length can be tuned by changing the size of the patch.** (A) Confocal images show that the 8- $\mu\text{m}$  patch exhibited a focal length six times larger ( $> 25 \mu\text{m}$ ) than that of the 3- $\mu\text{m}$  patch. Operating  $\lambda = 670 \text{ nm}$ . (B)  $z$ -linescans of the optical transmission patterns showed significant shift of the focal length as the size of the patches varied. Increasing the diameter of the patch also resulted in a long depth of focus ( $> 20 \mu\text{m}$ ). (C)  $x$ -linescans across the center of the focal planes showed that smaller patches exhibited foci with reduced lateral dimensions.